

1 **Modelling silicon supply during the Last Interglacial (MIS 5e) at Lake Baikal**

2 Panizzo, V.N.^{1,2}, Swann, G.E.A.^{1,2}, Mackay, A.W.³, Pashley, V.⁴, and Horstwood, M.S.A.⁴

3 ¹*School of Geography, University of Nottingham, University Park, Nottingham, NG7 2RD, UK*

4 ²*Centre for Environmental Geochemistry, University of Nottingham, University Park, Nottingham, NG7*
5 *2RD, UK*

6 ³*Environmental Change Research Centre, Department of Geography, University College London,*
7 *Gower Street, London, WC1E 6BT, UK*

8 ⁴*NERC Isotope Geosciences Laboratory, British Geological Survey, Keyworth, Nottingham, NG12 5GG,*
9 *UK*

10

11 *Corresponding author: virginia.panizzo@nottingham.ac.uk

12

13 **Abstract**

14 Limnological reconstructions of primary productivity have demonstrated its response over Quaternary
15 timescales to drivers such as climate change, landscape evolution and lake ontogeny. In particular,
16 sediments from Lake Baikal, Siberia, provide a valuable uninterrupted and continuous sequence of
17 biogenic silica (BSi) records, which document orbital and sub-orbital frequencies of regional climate
18 change. We here extend these records via the application of stable isotope analysis of silica in diatom
19 opal ($\delta^{30}\text{Si}_{\text{diatom}}$) from sediments covering the Last Interglacial cycle (Marine Isotope Stage [MIS] 5e; c.
20 130 to 115 ka BP) as a means to test the hypothesis that it was more productive than the Holocene.
21 $\delta^{30}\text{Si}_{\text{diatom}}$ data for the Last Interglacial range between +1.29 to +1.78‰, with highest values between c.
22 127 to 124 ka BP (+1.57 to +1.78‰). Results show that diatom dissolved silicon (DSi) utilisation, was
23 significantly higher ($p=0.001$) during MIS 5e than the current interglacial, which reflects increased
24 diatom productivity over this time (concomitant with high diatom biovolume accumulation rates [BVAR]
25 and warmer pollen-inferred vegetation reconstructions). Diatom BVAR are used, in tandem with
26 $\delta^{30}\text{Si}_{\text{diatom}}$ data, to model DSi supply to Lake Baikal surface waters, which shows that highest delivery
27 was between c. 123 to 120 ka BP (reaching peak supply at c. 120 ka BP). When constrained by
28 sedimentary mineralogical archives of catchment weathering indices (e.g. the Hydrolysis Index), data
29 highlight the small degree of weathering intensity and therefore representation that catchment-
30 weathering DSi sources had, over the duration of MIS 5e. Changes to DSi supply are therefore attributed

31 to variations in within-lake conditions (e.g. turbulent mixing) over the period, where periods of both high
32 productivity and modelled-DSi supply (e.g. strong convective mixing) account for the decreasing trend
33 in $\delta^{30}\text{Si}_{\text{diatom}}$ compositions (after c. 124 ka BP).

34

35 **Key words**

36 Eemian, Kazantsevo, diatoms, silicon isotopes, Siberia, palaeoproductivity

37

38 **1. Introduction:**

39 Primary productivity is a key ecosystem function synthesizing organic matter. In deep lakes production
40 is usually dominated by phytoplankton. Over long timescales, primary production is controlled by a
41 number of external and internal drivers such as climate change, landscape evolution and lake ontogeny.
42 Species composition also has an important influence on productivity-diversity relationships (e.g. Dodson
43 et al., 2000). On Quaternary timescales palaeoproductivity may be estimated using a number of different
44 techniques, including palaeoecological (e.g. diatom analysis) biogeochemical (e.g. biogenic silica or
45 pigment analysis) or stable isotope approaches. Palaeoproductivity records allow us to test key
46 hypotheses related to climate variability, including differences between interglacial periods, which may
47 act as analogues to a future warming world. One of the most studied interglacials is the Last Interglacial,
48 a possible analogue for a future, warmer Earth (although in terms of orbital configuration, this
49 comparison is imperfect).

50

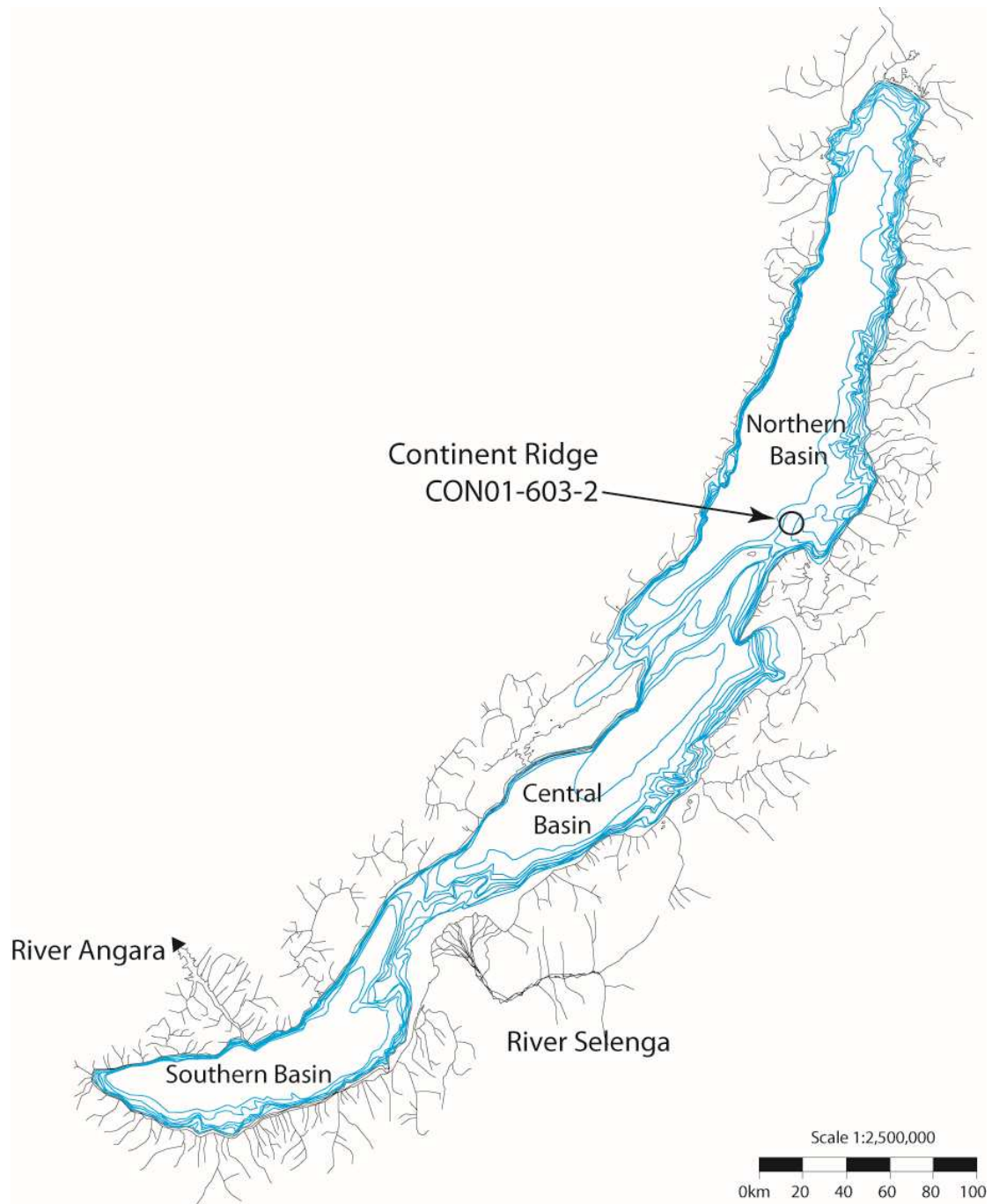
51 The Last Interglacial, corresponding to Marine Isotope Stage (MIS) 5e (130 - 115 ka BP; PAGES, 2016;
52 Railsback et al., 2015), is often referred to as the Eemian in Western European continental records, or in
53 Siberia, the Kazantsevo. In order to more fully understand the nature, duration and synchronicity of MIS
54 5e across the globe, the comparison of independent continental and oceanic climate records are needed.
55 Lake Baikal, Siberia (103°43'-109°58'E and 51°28'-55°47'N; Figure 1) provides a key uninterrupted,
56 continental sedimentary archive, which spans at least the past 20 million years (Williams et al., 2001), to
57 which further Eurasian continental records (e.g. loess sequences) can be compared (Prokopenko et al.,
58 2006). Lake Baikal is the world's deepest and most voluminous lake (23, 615 km²) with a catchment of
59 over 540, 000 km². Its mid-latitude location in central Asia means that the lake is highly continental

60 (Lydolph, 1977), and sensitive to obliquity- and precessional-driven forcing (Short et al., 1991), which
61 has allowed an astronomically tuned climate record for the entire Pleistocene (Prokopenko et al., 2006).

62

63 **Figure 1.**

64 Map of Lake Baikal and its catchment with core CON-01-603-2 drilling location identified.



65

66

67

68 Prokopenko et al. (2001) argued that biogenic silica (BSi) records from Lake Baikal register regional
69 climatic fluctuations (e.g. glacial-interglacial cycles) and are linked to incoming solar radiation (hereafter
70 insolation) forcing, via heat balance exchanges within the lake (e.g. Prokopenko et al., 2006; Prokopenko
71 et al., 2001). At sub-orbital frequencies, BSi concentration may be related to regional climate change,
72 linked to teleconnections with shifting Atlantic Meridional Overturning Circulation (e.g. Karabanov et
73 al., 2000). On orbital timescales, Lake Baikal BSi records are interpreted as a palaeoproductivity proxy
74 (Mackay, 2007; Prokopenko et al., 2006; Prokopenko et al., 2001). Seasonal phytoplankton succession
75 at Lake Baikal today is influenced by the timing of ice-off (end of May-June) and ice-on (after October),
76 which promote a period of rapid diatom growth via upper water column turbulent mixing (Popovskaya,
77 2000). The thermal regime of Lake Baikal in spring and autumn periods is therefore very important in
78 regulating diatom bloom development, together with the availability of dissolved silicon (DSi) (Panizzo
79 et al., in review; Popovskaya et al., 2015). While these productivity proxies (e.g. BSi, in tandem with
80 diatom assemblages) can provide an insight into variations in limnological characteristics (e.g. length of
81 growing season, lake turnover) over previous glacial-interglacial cycles, they do not provide the ability
82 to quantitatively assess variations between within-lake, versus catchment, delivery of nutrients (namely
83 DSi). We aim to address this in this study, via the use of silicon stable isotope geochemistry to reconstruct
84 such changes over the Last Interglacial.

85

86 There are three stable isotopes of silicon (Si: ^{28}Si , ^{29}Si and ^{30}Si), which fractionate during almost all low-
87 temperature processes of the continental and oceanic silicon cycles, highlighting their value as a
88 geochemical tracer. Variations in the isotope abundances (e.g. $^{30}\text{Si}/^{28}\text{Si}$ [although previously more
89 commonly $^{29}\text{Si}/^{28}\text{Si}$]) are reported via the delta notation ($\delta^{30}\text{Si}$), when compared to a known standard
90 reference material (e.g. NBS 28). Records of $\delta^{30}\text{Si}$ composition of waters and diatom opal ($\delta^{30}\text{Si}_{\text{DSi}}$ and
91 $\delta^{30}\text{Si}_{\text{diatom}}$ respectively) from Lake Baikal have demonstrated the clear relationship between diatom
92 biomass and nutrient availability (Panizzo et al., in review; Panizzo et al., 2017; Panizzo et al., 2016),
93 pointing to $\delta^{30}\text{Si}_{\text{diatom}}$ as a proxy for surface water DSi utilisation. This is because DSi (in the form of
94 silicic acid [$\text{Si}(\text{OH})_4$]) is a key nutrient for diatom uptake and growth (Martin-Jezequel et al., 2000).
95 During biomineralisation diatoms discriminate against the heavier isotopes (^{29}Si and ^{30}Si) over the lighter
96 (^{28}Si), which leads to the preferential isotopic enrichment of the residual solution (in this case, the
97 dissolved phase: $\delta^{30}\text{Si}_{\text{DSi}}$) in the heavier isotopes. This in turn leaves a clear biological imprint on the

98 isotopic composition of BSi (De La Rocha et al., 1997). The per mille fractionation or enrichment factor
99 (termed $^{30}\epsilon_{\text{uptake}}$) between both phases is considered to be between c. -1.1 and -1.6‰ (estimated from
100 freshwater systems; Alleman et al., 2005; Opfergelt et al., 2011; Panizzo et al., 2016; Sun et al., 2013)
101 and be independent of temperature, $p\text{CO}_2$ and nutrient availability (De La Rocha et al., 1997; Fripiat et
102 al., 2011; Milligan et al., 2004; Varela et al., 2004) some *in-vitro* studies on oceanic diatoms have
103 suggested a species dependent $^{30}\epsilon_{\text{uptake}}$ effect (Sutton et al., 2013). While this final attestation remains in
104 dispute, in the case of Lake Baikal *in-situ* estimations of diatom $^{30}\epsilon_{\text{uptake}}$ are c. -1.6‰ , derived from
105 calculations of seasonal BSi (Panizzo et al., 2016). A final important consideration is the preservation of
106 the $\delta^{30}\text{Si}_{\text{diatom}}$ in surface sediments, where it is estimated that only c. 1% of total diatom valves are
107 preserved in Lake Baikal (Ryves et al., 2003). Despite this being a pervasive issue at this site, Panizzo et
108 al. (2016) demonstrate the absence of any diatom dissolution associated $^{30}\epsilon$ (as per earlier studies by
109 Demarest et al., 2009) and therefore validate the application of $\delta^{30}\text{Si}_{\text{diatom}}$ reconstructions from lake
110 sediments.

111

112 On the basis of the above discussion and earlier work at Lake Baikal (Panizzo et al., In review; Panizzo
113 et al., 2017; Panizzo et al., 2016), we propose that $\delta^{30}\text{Si}_{\text{diatom}}$ sedimentary records can act as a tracer of
114 past diatom nutrient uptake. In addition, we apply silicon isotope geochemistry from Lake Baikal
115 sediments as a means to explore, in more detail, the catchment and within-lake constraints on silicon
116 cycling (via the application of independent diatom productivity proxies), as a means to understand how
117 climate has impacted nutrient supply, productivity and export at Lake Baikal over MIS 5e. Our objectives
118 are to provide, firstly, an overview of $\delta^{30}\text{Si}_{\text{diatom}}$ signatures in MIS 5e and determine if diatom utilisation
119 was higher than the current interglacial. Secondly, to reconstruct palaeo-nutrient supply of DSi in Lake
120 Baikal surface waters over the course of the Last Interglacial. In particular, we compare these parameters
121 with existing palaeolimnological proxies the better to reconstruct variations in nutrient availability and
122 diatom uptake, as a response to prevailing orbital and climatological changes. Finally we devise a new
123 interpretive model to best describe intra-Last Interglacial variability at Lake Baikal.

124

125 **2. Materials and methods:**

126 **2.1. Core collection**

127 Core CON-01-603-2 was collected on the Continent Ridge, north basin, of Lake Baikal in July 2001 at
128 the location of 53°57' N, 108°54' E (Figure 1). The core was collected from a water depth of 386 m
129 using a piston corer, with full details provided by Demory et al. (2005a); Demory et al. (2005b) Charlet
130 et al. (2005). Detailed summaries on CON-01-603-2 core collection and chronology (radiocarbon and
131 palaeomagnetism) can be found therein. Sample resolution represents c. 200 years for the majority of the
132 record, although this increases to c. 400 years between 118 ka to 116 ka BP.

133

134 Here we present the methods for this new data set of $\delta^{30}\text{Si}_{\text{diatom}}$ alone, although reference is also made to
135 existing datasets of $\delta^{18}\text{O}_{\text{diatom}}$ (Mackay et al., 2013), diatom biovolume accumulation rates (BVAR)
136 (Rioual and Mackay, 2005), catchment weathering indices (e.g. sediment clay mineralogy; Fagel and
137 Mackay, 2008) and pollen-derived vegetation biome reconstructions (Tarasov et al., 2005; derived from
138 the pollen reconstructions of Granoszewski et al., 2005) from the same core (Figures 3,4).

139

140 **2.2. Silicon isotope preparation and analysis**

141 A total of 16 samples for $\delta^{30}\text{Si}_{\text{diatom}}$ analyses were selected across an existing $\delta^{18}\text{O}_{\text{diatom}}$ record (Mackay
142 et al., 2013) from sediment core CON-01-603-2. Samples underwent preparation to remove high episodes
143 of contamination (namely Al_2O_3) via more vigorous cleaning (of the existing diatom opal from Mackay
144 et al., 2013), including heavy density separation and organic material oxidation (as per methods outlined
145 in Morley et al., 2004). Prior to isotopic analysis, all samples were visually inspected via a Zeiss Axiovert
146 40 C inverted microscope, while X-ray fluorescence (XRF) analyses were also conducted in order to
147 verify, quantitatively, their purity. All samples demonstrated no visual contamination (e.g. clay) and
148 quantitative estimations via XRF are <1% (with sample $\text{Al}_2\text{O}_3/\text{SiO}_2 < 0.01$).

149

150 Alkaline fusion (NaOH) of cleaned diatom opal and subsequent ion-chromatography (via cation
151 exchange methods; BioRad AG50W-X12) followed methodologies outlined by Georg et al. (2006), with
152 further analytical and methodological practices mentioned in Panizzo et al. (2016). Samples were
153 analysed in wet-plasma mode using the high mass-resolution capability of a ThermoScientific Neptune
154 Plus MC-ICP-MS (multi collector inductively coupled plasma mass spectrometer) at the British
155 Geological Survey. A minimum of two analytical replicates were made per sample. Full analytical
156 methods are detailed in Panizzo et al. (2017; 2016), including practices applied to minimize instrument

157 induced mass bias and drift (e.g. Cardinal et al., 2003; Hughes et al., 2011). Full procedural blank
158 compositions from MC-ICP-MS analyses were 31 ng compared to typical fusion amounts of 3390 ng
159 and differed from sample compositions by < 0.5%. Using the worst-case scenario (i.e. calculated using
160 the sample with the lowest Si concentration) this level of blank could result in a potential shift in sample
161 composition by < 0.04‰. All blank measurements therefore demonstrated an insignificant effect relative
162 to the typical < 0.11‰ propagated sample uncertainties (Table 1) and no correction for procedural blank
163 was made.

164

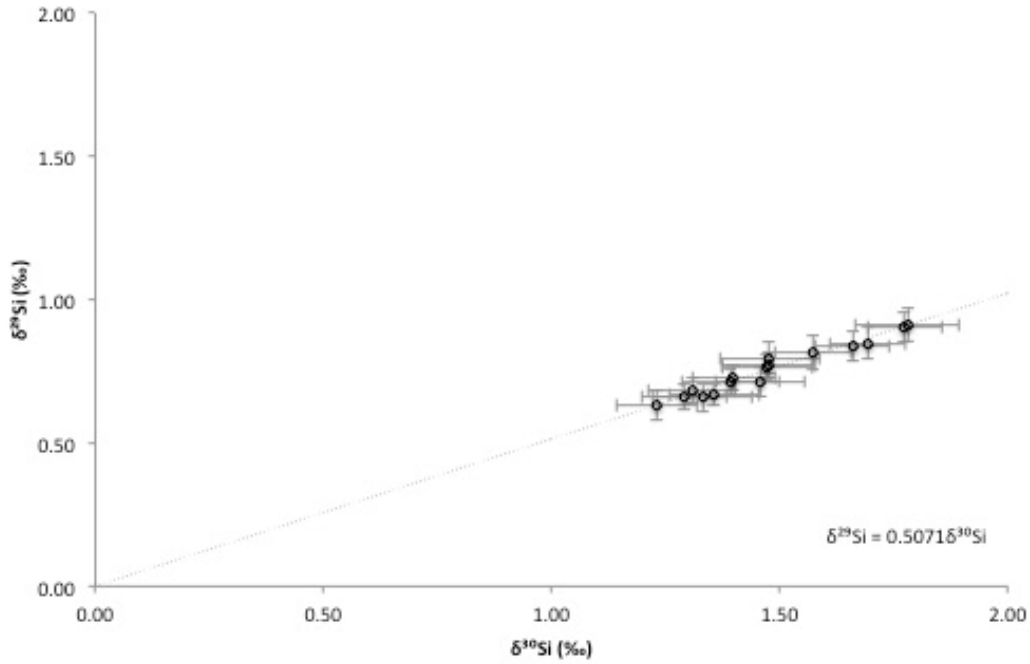
165 All uncertainties are reported at 2 sigma absolute (Table 1), and incorporate an excess variance derived
166 from the NBS 28 reference material, which was quadratically added to the analytical uncertainty of each
167 measurement. $\delta^{29}\text{Si}$ and $\delta^{30}\text{Si}$ were compared to the mass dependent fractionation line to which all
168 samples comply (Figure 2). Long term (~ 2 years) reproducibility and machine accuracy are assessed via
169 analyzing the Diatomite secondary standard and data agree with the published values: Diatomite =
170 $+1.24\text{‰} \pm 0.18\text{‰}$ (2 SD, n=244) (consensus value of $+1.26\text{‰} \pm 0.2\text{‰}$, 2 SD; Reynolds et al., 2007).

171

172 **Figure 2.**

173 Three-isotope plot ($\delta^{29}\text{Si}$ vs $\delta^{30}\text{Si}$) for all silicon isotope data (n=16) presented in this manuscript, with
174 data falling within analytical uncertainty of the mass-dependent fractionation line (dashed); in good
175 agreement with the kinetic fractionation of Si of 0.5092 (Reynolds et al., 2007).

176



177

178

179

180 2.3. Modelling palaeo-surface water nutrient availability

181 Based on an open system model approach (Eq. 1), which is considered most appropriate at Lake Baikal

182 (Panizzo et al., 2017), the equation can be re-arranged to calculate palaeo %DSi_{utilisation} (Eq. 2):

183

$$184 \quad \delta^{30}\text{Si}_{\text{DSi}} = \delta^{30}\text{Si}_{\text{initial}} - {}^{30}\epsilon_{\text{uptake}} (1 - f_{\text{Si}}) \quad \text{Eq. 1}$$

$$185 \quad \% \text{DSi}_{\text{utilisation}} = 1 - [(\delta^{30}\text{Si}_{\text{diatom}} - \delta^{30}\text{Si}_{\text{initial}}) / -{}^{30}\epsilon_{\text{uptake}}] \quad \text{Eq. 2}$$

186

187 Where $\delta^{30}\text{Si}_{\text{initial}}$ is the initial composition of the dissolved pool, before biological enrichment. We argue

188 that this acts as baseline surface water compositions when ice-off and turbulent mixing occurs, leading

189 to the first (larger) spring diatom bloom (Panizzo et al., 2017). Modern day deep water (>500m)

190 compositions from Lake Baikal vary between +1.71‰ and +1.77‰ (data derived from the south and

191 north basins respectively) (Panizzo et al., 2017). Taking into consideration a 2SD on these values (0.04‰

192 and 0.03‰ respectively), a maximum and minimum likelihood $\delta^{30}\text{Si}_{\text{initial}}$ composition can be calculated

193 and a 95% confidence interval applied to modelled DSi utilization (Figures 3; 4). The assumption that

194 modern day $\delta^{30}\text{Si}_{\text{initial}}$ can be applied here may lead to some uncertainty in %DSi_{utilisation} estimations (e.g.

195 >100%; Table 1) however, in the absence of palaeo- $\delta^{30}\text{Si}_{\text{initial}}$ compositions from Lake Baikal we argue

196 its application here. $\delta^{30}\text{Si}_{\text{diatom}}$ is the isotopic composition of diatom opal at any given time interval and
197 $^{30}\epsilon_{\text{uptake}}$ is set at -1.6% , as discussed in Section 1 (Panizzo et al., 2017; Panizzo et al., 2016).

198

199 In addition to simply quantifying past DSi surface utilisation via diatom biomineralisation, here we aim
200 to reconstruct palaeo-nutrient supply in Lake Baikal. As independent diatom productivity indicators (e.g.
201 BVAR) are also available from core CON-01-603-2, (Rioual and Mackay, 2005), an estimate of DSi
202 supply can be made by constraining $\delta^{30}\text{Si}_{\text{diatom}}$ compositions by the net export of BSi to sediments (e.g.
203 as a function of export production or nutrient demand; Horn et al., 2011). This application has been seen
204 in oceanic settings as a method to constrain better, reconstructions of nutrient supply, when coupled with
205 other algal productivity indicators (Horn et al., 2011).

206

$$207 \quad DSi \text{ Supply} = \frac{F_{BVAR}^{sample} / F_{BVAR}^{120.5 ka}}{\%DSi_{consumed}^{sample} / \%DSi_{consumed}^{120.5 ka}} \quad \text{Eq. 3}$$

208

209 F_{BVAR}^{sample} is the flux of BVAR in sediments and $\%DSi_{consumed}^{sample}$ is the percentage of the DSi consumed by
210 diatoms (in the sediment record). $F_{BVAR}^{120.5 ka}$ and $\%DSi_{consumed}^{120.5 ka}$ are defined as the sample with the greatest
211 modelled supply in the MIS 5e record (at c. 120.5 ka BP; Table 1). We apply the use of BVAR here (over
212 %BSi) as we argue this reflects more realistically the DSi demand of diatoms. Diatom BVAR take into
213 consideration diatom size (e.g. volume) and cell concentration, and so the amount of DSi biomineralised
214 in the valve (refer to Rioual and Mackay, 2005, for full explanation of calculation). Diatom dissolution
215 (defined as the percentage of pristine valves, of those preserved within the Lake Baikal record; Rioual
216 and Mackay, 2005; Table 1) across the MIS 6 to MIS 5d record is also consistently $<23\%$, which supports
217 the application of the proxy for modelling palaeo-DSi supply; i.e. ruling out that dominant BVAR
218 changes over this time over this record are a function of diatom dissolution. BSi records on the other
219 hand represent bulk biogenic opal in sediments, which has evaded remineralisation (e.g. Ryves et al.,
220 2003) and may not be exclusively diatomaceous in origin (e.g. catchment derived amorphous silica).
221 Zonation of Figure 4 and the discussion surrounding the conceptual model at Lake Baikal (Section 4.2;
222 Figure 5) is based on the Diatom Assemblage Zonations (DAZ) defined by Rioual and Mackay (2005).

223

224 **3. Results:**

225 The data set presented here starts at the end of Termination 2 (c. 132 ka BP, n=1) through to the transition
226 from MIS 5e to MIS 5d at c. 116 ka BP. The resolution of sampling is at the millennial-scale, c. every
227 850 years. All $\delta^{30}\text{Si}_{\text{diatom}}$ data range between +1.23 and +1.78‰ (0.17‰ 1SD of all final data, n=16;
228 Table 1). Lowest $\delta^{30}\text{Si}_{\text{diatom}}$ compositions are seen at c. 132.1 ka BP ($+1.23 \pm 0.09\text{‰}$, n=1; Table 1),
229 during zone MIS 6. Highest values (between $+1.77 \pm 0.08\text{‰}$ and $+1.48 \pm 0.11\text{‰}$, n=7; Table 1) are
230 demonstrated in early MIS 5e (c. 127.4 and 123.0 ka BP), with a progression to lower values (c. $1.47 \pm$
231 0.1‰ and $+1.30 \pm 0.10$, n=8; Table 1) between c. 122.0 and 116.1 ka BP (Figure 3). There is one episode
232 of lower signatures, outside of the general MIS 5e decreasing trend, between c. 127.4 and 126.8 ka BP,
233 where values fall to $+1.46 \pm 0.1\text{‰}$ (at c. 126.8 ka BP).

234

235 The linear approximation (via open system/steady state modelling) of DSi supply is portrayed in Table
236 1 and Figure 4. Percentage results are relative to the sample that has the highest modelled supply in the
237 record (e.g. 100% at c. 120.5 ka BP; Table 1). Results show an average c. 70% supply (range between c.
238 64 and c. 100% over the period of MIS 5e) (e.g. c. 30% less supply that at 120.5 ka BP) after the
239 termination of the previous glacial MIS 6 (Figure 4). There is a step increase in modelled supply during
240 MIS 5e, after c. 124.9 ka, which is coincident with the continued decreasing trend in $\delta^{30}\text{Si}_{\text{diatom}}$ signatures
241 and estimated %DSi utilisation over the course of the Last Interglacial (Figure 4).

242

243

244

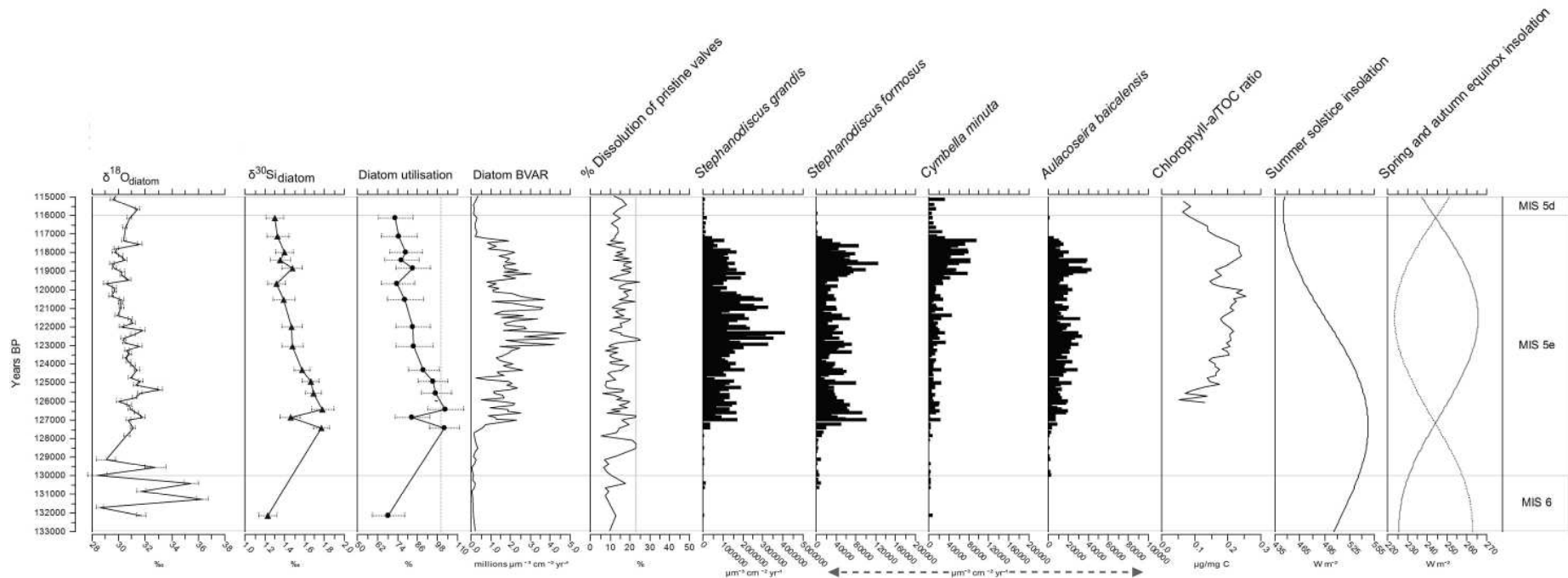
245 **Table 1**

246 $\delta^{30}\text{Si}_{\text{diatom}}$ and $\delta^{29}\text{Si}_{\text{diatom}}$ data (n=16) reported for the period 132.15 ka BP and 116.16 ka BP, with respective 2 sigma absolute analytical errors (‰). Sample names are provided
 247 in tandem with the modelled respective ages (ka BP) and mid-sediment sampling depth (CON-01-603-2). Data are presented with published total biovolume (millions μm^{-3}
 248 $\text{cm}^{-2} \text{year}^{-1}$) and % diatom dissolution index (Rioual and Mackay, 2005) data. The modelled open system %DSi utilisation and %DSi Supply (including maximum and minimum
 249 modelled likelihood errors) for each sample are also given.

Sample Name	Mid-sediment depth (cm)	Dating profile (ka BP)	$\delta^{30}\text{Si}_{\text{diatom}}$ (‰)	± 2 sigma absolute (‰)	$\delta^{29}\text{Si}_{\text{diatom}}$ (‰)	± 2 sigma absolute (‰)	Biovolume (millions $\mu\text{m}^{-3} \text{cm}^{-2} \text{year}^{-1}$)	% Valve dissolution index	Modelled DSi Utilisation (%)	\pm Likelihood error (%)	Modelled DSi Supply (%)	\pm Likelihood error (%)
EEM_12	613	116.16	+1.29	0.09	+0.66	0.04	0.27	15	73	11	9	1
EEM_14	617	117.17	+1.33	0.11	+0.66	0.05	0.18	13	75	11	6	1
EEM_18	625	118.00	+1.40	0.09	+0.73	0.04	1.81	13	79	10	59	8
EEM_20	629	118.42	+1.36	0.10	+0.67	0.04	1.51	12	76	11	50	8
EEM_22	633	118.84	+1.47	0.10	+0.77	0.05	1.39	21	83	11	43	6
EEM_26	641	119.68	+1.31	0.09	+0.68	0.05	1.05	18	74	11	36	6
EEM_30	649	120.53	+1.39	0.11	+0.72	0.04	3.06	15	78	11	100	16
EEM_37	663	122.00	+1.47	0.10	+0.76	0.05	2.21	16	83	11	68	9
EEM_42	673	123.05	+1.48	0.11	+0.80	0.06	1.23	9	84	11	38	5
EEM_48	685	124.32	+1.57	0.08	+0.81	0.06	2.12	16	90	9	61	7
EEM_51	691	124.95	+1.66	0.08	+0.84	0.05	1.56	8	95	9	42	4
EEM_54	697	125.58	+1.69	0.08	+0.85	0.06	1.01	6	97	9	27	3
EEM_58	705	126.42	+1.78	0.11	+0.91	0.06	1.55	10	102	11	39	4
EEM_60	709	126.85	+1.46	0.10	+0.72	0.05	1.02	23	82	11	32	4
EEM_62	713	127.44	+1.77	0.08	+0.90	0.05	0.47	15	102	9	12	1
EEM_73	735	132.15	+1.23	0.09	+0.63	0.05	0.11	13	68	10	4	1

250

251



252

253

254

Figure 3.

255 Stratigraphic plot displaying $\delta^{18}\text{O}_{\text{diatom}}$ (‰) from Mackay et al. (2013) (note that data before c. 128 ka BP are not plotted due to contamination issues outlined by the authors),
 256 $\delta^{30}\text{Si}_{\text{diatom}}$ (‰) with respective analytical errors, modelled %DSi utilisation (95% confidence intervals shown) from this dataset (open system model), total diatom biovolume
 257 accumulation rates (BVAR) (millions $\mu\text{m}^{-3}\text{cm}^{-2}\text{yr}^{-1}$) (Rioual and Mackay, 2005), % valve dissolution index (defined as the percentage of pristine valves, of those preserved
 258 within in the record; Table 1) (Rioual and Mackay, 2005), dominant diatom species BVAR (thousands/millions $\mu\text{m}^{-3}\text{cm}^{-2}\text{yr}^{-1}$) (Rioual and Mackay, 2005), Chlorophyll
 259 *a*/TOC data ($\mu\text{g}/\text{mg C}$; Fietz et al., 2007) and insolation at 55°N (W m^{-2}) for the summer solstice and winter, spring (dashed) equinoxes. All sediment core proxies presented
 260 are derived from core CON-01-603-2 (Figure 1).

261

262 4. Discussion

263 4.1. $\delta^{30}\text{Si}_{\text{diatom}}$ signatures during MIS 5e

264 The main focus of this discussion spans the MIS 5e period, although one data point of the record is
265 derived from the MIS 6 glacial (before c. 130 ka BP; Table 1, Figure 3). The ranges of values presented
266 here (from sediments collected from the North Basin; Figure 1) ($+1.23$ to $+1.78 \pm 0.17\%$; Table 1)
267 encompass mean modern day south basin surface sediment $\delta^{30}\text{Si}_{\text{diatom}}$ signatures ($+1.23\% \pm 0.08$ 1 SD;
268 Panizzo et al., 2016), especially the MIS 6 value. The $\delta^{30}\text{Si}_{\text{diatom}}$ data presented over MIS 5e (in particular
269 c. 127.4 ka BP to c. 116 ka BP) displays an overall decreasing trend concomitant, and significantly
270 correlated with, the decrease in June (solstice) insolation (at 55°N) ($r^2=0.53$, $p=0.001$). However, there
271 is an absence of correlation between $\delta^{30}\text{Si}_{\text{diatom}}$ and insolation (at 55°N) records of each spring and autumn
272 equinoxes (Figure 3) or winter solstice (data not shown). Furthermore, Last Interglacial $\delta^{30}\text{Si}_{\text{diatom}}$ values
273 (between $+1.30 \pm 0.10\%$ and $+1.77 \pm 0.08\%$; Table 1) are significantly higher than Holocene $\delta^{30}\text{Si}_{\text{diatom}}$
274 compositions (Panizzo et al, unpublished data) derived from sediment cores across all three Lake Baikal
275 basins ($p=0.001$, via a Kruskal Wallis test).

276

277 Palaeoecological records in the Lake Baikal suggest that the climate was warmer and wetter during the
278 Last Interglacial than the Holocene (Tarasov et al., 2007), which in turn may account for the higher
279 $\delta^{30}\text{Si}_{\text{diatom}}$ -inferred utilisation over this period (Figure 3). Given the significantly higher $\delta^{30}\text{Si}_{\text{diatom}}$
280 signatures for MIS 5e we can interpret this as a period of either higher utilisation of DSi by diatoms (e.g.
281 enhanced productivity) and/or a weakened supply of nutrients to the surface (e.g. reduced convective
282 mixing or catchment derived nutrients). These arguments will be discussed further in the following
283 section, in conjunction with other climate and productivity indicators from Lake Baikal during MIS 5e.

284

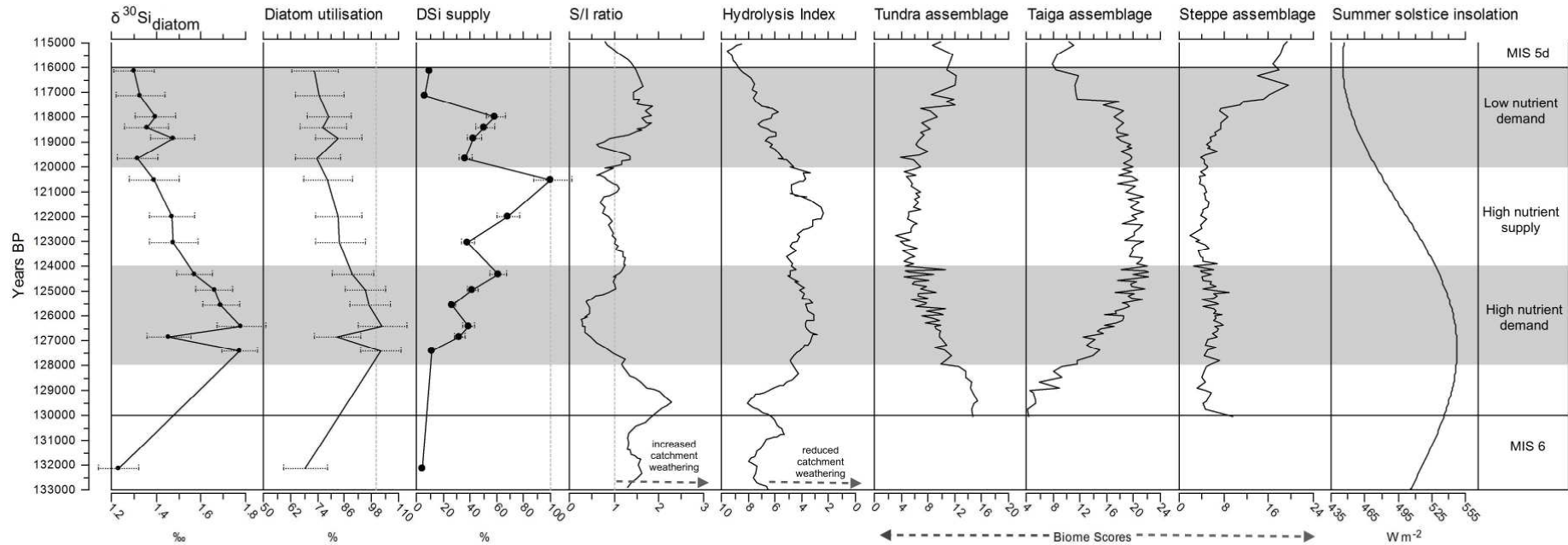
285

286

287
288
289
290
291
292

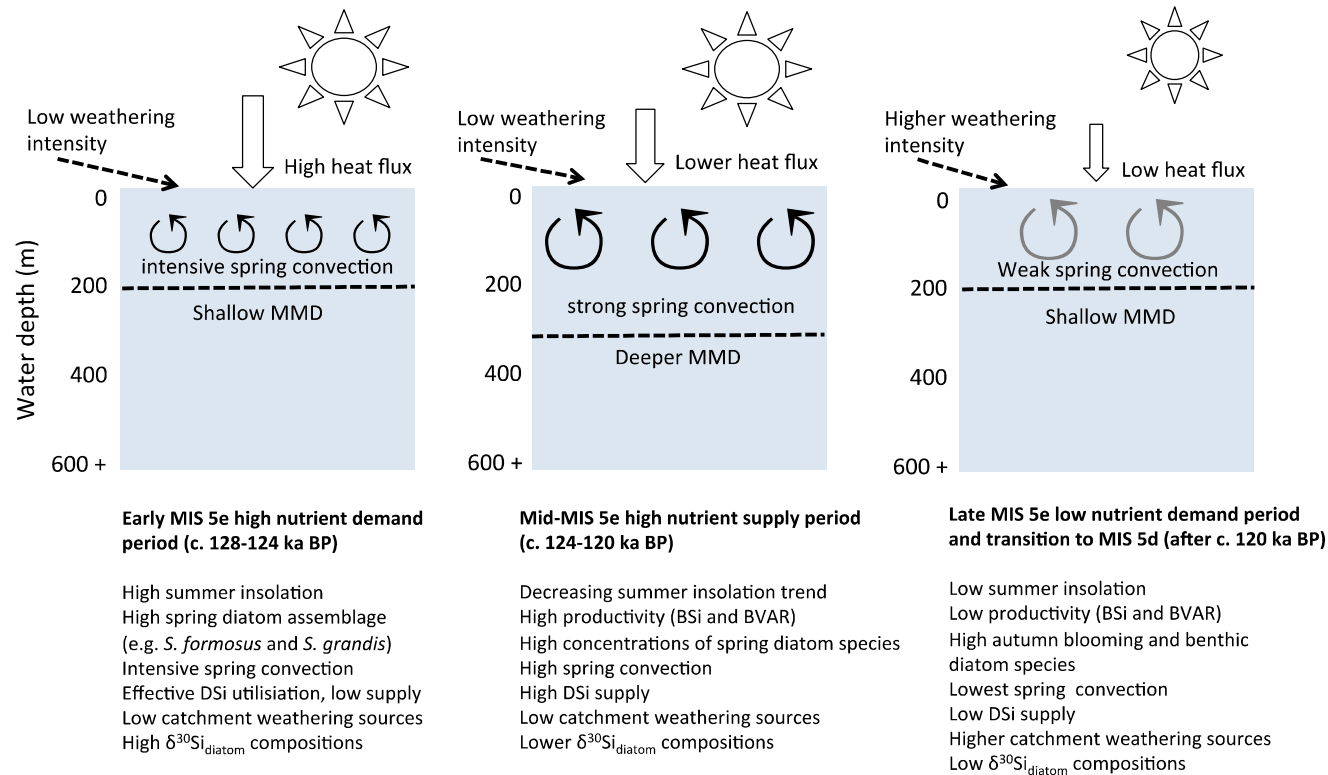
Figure 4.

Summary diagram of $\delta^{30}\text{Si}_{\text{diatom}}$ (‰) with respective analytical errors, modelled %DSi utilisation and estimated %DSi supply (with 95% confidence intervals), both constrained by BVAR. S/I ratios and the Hydrolysis Index (note reverse axis) (Fagel et al., 2005), along with dominant catchment biome scores (Tarasov et al., 2005) and summer solstice insolation at 55°N (W m^{-2}) are also displayed. Lines correspond to the time transition from MIS 6 to MIS 5e and MIS 5d. Shaded areas correspond to the interpretation of lake nutrient cycling as described in Section 4.2 and Figure 5 (defined as the DAZ of Rioual and Mackay, 2005).



293
294
295
296

297 **Figure 5.** A schematic nutrient-productivity model for the Lake Baikal upper water column (including surface waters to the MMD), during the Last Interglacial. Three
 298 interpretive periods are identified (Section 4.2) for MIS 5e and a description of the dominant drivers of upper water column nutrient availability (e.g. catchment versus within-
 299 lake) are provided. A summary of the dominant palaeoecological characteristics of these periods is also provided (based on Figures 3, 4), along with the main climatic forcing
 300 (e.g. insolation).
 301



302 **4.2. A conceptual model of diatom responses to altering DSi supply during the Last Interglacial**

303 A hydrodynamic-insolation model for the Lake Baikal BSi signal was proposed by Prokopenko et al.
304 (2001), where two models were put forward for diatom productivity during either interglacial (high
305 insolation and high BSi) or glacial (low insolation and low BSi) stages. However, as intra-Last
306 Interglacial climate variability has been demonstrated (including cooling; Karabanov et al., 2000;
307 atmospheric circulation and hydrological regime changes in the catchment; Mackay et al., 2013; and
308 changes in primary productivity; Rioual and Mackay, 2005), we here propose a more sensitive
309 interpretation via the application of diatom BVAR (Section 2.3; Figure 5). This revised nutrient-
310 productivity model reflects the variation captured in both diatom utilisation and nutrient (DSi) supply
311 over the course of MIS 5e (Figure 4), which was otherwise not accounted for in earlier models (e.g.
312 Prokopenko et al, 2001).

313

314 For the purpose of this discussion, we consider the delivery of nutrients (DSi) from both within-lake
315 (upwelling) and catchment derived processes. The Hydrolysis Index (HI) (Figure 4) of Fagel and Mackay
316 (2008) can be used to examine catchment weathering in Lake Baikal as a function of climatic conditions,
317 parent rock type and catchment topography (Fagel and Boes, 2008). Higher values (>5) therefore indicate
318 a greater presence of secondary minerals (e.g. increased weathering), while lower values are indicative
319 of primary mineral clay sources in sediments (e.g. reduced catchment weathering). Meanwhile,
320 smectite/illite ratios (S/I) are indicative of increased chemical weathering (>1) or increased physical
321 catchment weathering (<1), with illite being defined as one parent mineral endmember for the site (Fagel
322 and Mackay, 2008). In terms of silicon geochemistry, chemical weathering of silicate rocks and minerals
323 are attributable to the DSi load of rivers and ultimately lakes and oceans (e.g. Stumm and Wollast, 1990)
324 however physical erosion, controlled by climate, soil formation and catchment vegetation, can also play
325 an important role in deriving continental DSi fluxes (Gaillardet et al., 1999). Under low erosion rates,
326 weathering is regarded to be supply-limited; so that clay mineral formation is higher (than primary
327 mineral dissolution), which will reduce DSi fluxes (relative to parent material)(e.g. low DSi/[Na+K]*;
328 Fontorbe et al., 2013; Frings et al., 2015; Hughes et al., 2013) and preferentially discriminate against the
329 heavy isotopes (indicative of higher river $\delta^{30}\text{Si}_{\text{DSi}}$ signatures). This interpretation is referred to as
330 incongruent weathering (refer to the comprehensive discussion of Frings et al., 2016 and references
331 therein). The opposite scenario (kinetic-limited or more congruent weathering) occurs under higher

332 physical erosion rates (e.g. low weathering intensity [W/D]; Bouchez et al., 2014), where the rapid
333 removal of material and low riverine/sedimentary residence times reduces the accumulation of secondary
334 mineral phases (high $\text{DSi}/[\text{Na}+\text{K}]^*$, higher DSi fluxes and lower river $\delta^{30}\text{Si}_{\text{DSi}}$ signatures).

335

336 Quantitative catchment reconstructions of palaeo-weathering fluxes and DSi inflow compositions to
337 Lake Baikal are limited here due to the absence of catchment or riverine endmembers (from MIS 5e).
338 The overall need to expand silicon isotope continental paleo-weathering reconstructions has been
339 highlighted by Frings et al. (2016), although the greatest interest to date centers on quantifying river
340 $\delta^{30}\text{Si}_{\text{DSi}}$ signature variation to oceans (e.g. continental export) over glacial-interglacial cycles. Given that
341 the global river $\delta^{30}\text{Si}_{\text{DSi}}$ signatures exported to the ocean, between glacial-interglacial cycles, are
342 modelled to be only small e.g. estimated globally to increase only c. $0.2 \pm 0.25\%$ since the Last Glacial
343 Maximum following a reduction in weathering congruency (Frings et al., 2016) it is probable that intra-
344 Eemian variability of weathering regimes also has a small impact on altering Lake Baikal source waters
345 over this time. However, we here use the HI and S/I ratio of Fagel and Mackay (2008) as an independent
346 palaeo-weathering proxy to explore this argument and constrain any catchment derived sources of DSi
347 for diatom biomineralisation.

348

349 Three descriptive zones (derived from the DAZ of Rioual and Mackay, 2005; shaded in Figure 4) are
350 applied to examine variations in $\delta^{30}\text{Si}_{\text{diatom}}$ over the Last Interglacial, as a response to regional climate
351 changes and insolation forcing (Figure 5). We propose that while catchment changes (e.g. biome shifts
352 and weathering rates) may have played a role in regulating catchment DSi supply into Lake Baikal waters
353 (via rivers) over the course of MIS 5e (Figure 4), these act as more mediated responses. Rather we
354 propose that, as today, within-lake processes (reduced lake ice duration and increased turbulent,
355 convective mixing) are more rapid responses to, and therefore act as, the dominant driver in controlling
356 surface waters nutrient change over this time. Below we present a palaeoecological interpretation of the
357 three descriptive zonations (for MIS 5e alone), to which we propose this new interpretation of diatom
358 and nutrient responses over this period (Figure 5).

359

360 *4.2.1. Early MIS 5e high nutrient demand period (c. 128-124 ka BP):*

361 The increase to higher $\delta^{30}\text{Si}_{\text{diatom}}$ signatures in MIS 5e (after c. 127.4 ka BP) occurs at peak summer
362 insolation and is also coincident with the increase in diatom BVAR (Rioual and Mackay, 2005) and BSi
363 records (derived from different composite cores from the Academician Ridge; Prokopenko et al., 2006)
364 and later (after c. 126 ka BP) Chlorophyll-*a* (Figure 3). Mackay et al. (2013) interpret $\delta^{18}\text{O}_{\text{diatom}}$ data to
365 reflect a period of increased river discharge to Lake Baikal, in response to regional warming (increased
366 pollen-inferred precipitation and temperatures; Tarasov et al., 2007; Tarasov et al., 2005), a weaker
367 Siberian High (Velichko et al., 1991) and teleconnections with the North Atlantic (lowest global ice
368 volume; Kukla et al., 2002; and warmer North Atlantic sea surface temperatures; Oppo et al., 2006).
369 Apart from a brief reduction in $\delta^{30}\text{Si}_{\text{diatom}}$ signatures to +1.46‰ (± 0.10 2 sigma) at c. 126.8 ka BP, values
370 otherwise remain high during this period.

371

372 Both HI and S/I ratios are low after c. 128 ka BP (after a decreasing trend at the start of MIS 5e; Figure
373 4), which is indicative of physical (over chemical) weathering processes dominating in the catchment,
374 with limited secondary mineral formation in soils (e.g. low weathering intensity and higher proportion
375 of primary minerals in lake sediments) (Fagel and Mackay, 2008). During this period, these conditions
376 are concomitant with high summer insolation (Figures 4; 5) and an increase taiga biome scores, indicative
377 of a warming climate (Tarasov et al., 2007; Tarasov et al., 2005). Although the low S/I ratios (the lowest
378 in the record during this period) highlight changes in sediment clay mineralogy, which are a result of soil
379 destabilization in the catchment (Fagel and Mackay, 2008), the low HI is indicative of a low weathering
380 intensity regime (with probable low fractionation potential of river waters). This interpretation compares
381 well with BVAR-modelled DSi supply, which is among the lowest of the whole record (40-90% less
382 than peak supply at c. 120.5 ka BP; Table 1). Taken together these data suggest that the magnitude of
383 change to catchment DSi source waters was not great enough to alter considerably, pelagic source waters,
384 so that the high $\delta^{30}\text{Si}_{\text{diatom}}$ signatures are driven more strongly by diatom biomineralisation.

385

386 During the “high nutrient demand period” (c. 128 to 124 ka BP), spring blooming species *Stephanodiscus*
387 *formosus* and *Stephanodiscus grandis* (the latter which contributes the greatest to diatom BVAR; Figure
388 3) also increase, along with other *Aulacoseira baicalensis* and *Aulacoseira skvortzowii* species (Rioual
389 and Mackay, 2005). Although these *Stephanodiscus* species are today extinct, based on modern
390 analogues, Rioual and Mackay (2005) attribute them to be slow growing due to their large size, tolerant

391 of low light conditions with a high phosphorus and moderate silica demand, associated today with long
392 deep convective spring mixing (up to 300 m; Shimaraev et al., 1993). These data point to the
393 interpretation of enhanced nutrient exchange in surface waters at the beginning of MIS 5e, and a
394 productive initial spring diatom bloom, dominated by the high phosphorus, moderate DSi, nutrient
395 demand *Stephanodiscus* species (Figures 3,4). With low-modelled DSi supply over this period (including
396 from catchment sources), $\delta^{30}\text{Si}_{\text{diatom}}$ compositions become more enriched with an overall switch to
397 higher diatom productivity (BVAR; Figures 3, 4) and DSi utilisation, following MIS 6.

398

399 4.2.2. Mid-MIS 5e high nutrient supply period (c. 124-120 ka BP)

400 Estimated DSi utilisation is low after c. 124 ka BP, suggesting more nutrient rich conditions, concomitant
401 with the decreasing trend in $\delta^{30}\text{Si}_{\text{diatom}}$ signatures and step shift in higher diatom BVAR (Figure 4). This
402 trend also follows the decreasing summer insolation and $\delta^{18}\text{O}_{\text{diatom}}$ compositions (Figures 3, 4), although
403 the catchment is composed of a stable taiga biome (Figure 4; Tarasov et al., 2007; Tarasov et al., 2005).
404 Clay mineralogy (S/I ratio) during this zone continues to suggest conditions indicative of physical (over
405 chemical) weathering, with sediments dominated by primary mineral sources (low HI; Figure 4) and
406 therefore low chemical weathering in the catchment over this period. We interpret the record therefore
407 to point to a continued low weathering intensity (Section 4.2.1). As Lake Baikal catchment conditions
408 appear relatively stable during this zone (based on pollen and clay mineralogy) but modelled DSi supply
409 increases (Figure 4), which we suggest is due to within-lake DSi sources (e.g. increased mixing) being
410 more important in driving lower $\delta^{30}\text{Si}_{\text{diatom}}$ signatures (i.e. increased supply versus reduced diatom
411 uptake) rather than an increased catchment derived source of DSi (e.g. of lower $\delta^{30}\text{Si}_{\text{DSi}}$ composition).

412

413 Estimated supply increases during this period (c. 124 to 120 ka BP) reaching the time of highest modelled
414 supply (100%) at 120.5 ka BP (Table 1), concomitant with highest diatom BVAR and increased
415 Chlorophyll-*a* concentrations (Fietz et al., 2007) (Figure 3). The increase in diatom BVAR is again
416 attributed to the increase in *S. grandis* species (Rioual and Mackay, 2005), which proportionally
417 dominates diatom biovolumes over MIS 5e. We propose (based on modern-analogue diatom ecology) a
418 shift towards a deeper mesothermal maximum depth (MMD; Figure 5), concomitant with a deeper spring
419 mixing layer compared to the previous period. This will account for the increase in DSi supply to surface

420 waters and therefore some of the lowest $\delta^{30}\text{Si}_{\text{diatom}}$ compositions in the reconstruction, despite increased
421 diatom productivity.

422

423 4.2.3 Low nutrient demand period and the transition to MIS 5d (after 120 ka BP)

424 After c. 120.4 ka BP Rioual and Mackay (2005) document a notable change in individual diatom species
425 BVAR at Lake Baikal, from the large-celled *Stephanodiscus* species to smaller celled *Cyclotella* species,
426 especially *Cyclotella minuta* (Figures 3; 5). *C. minuta* can tolerate relatively high summer surface water
427 temperatures (e.g. during stratification), so that when autumnal mixing begins they are among the first
428 species to bloom (Jewson et al., 2015). These species changes are concomitant with a stepwise decrease
429 in total diatom BVAR, which points to a decrease in overall diatom productivity in Lake Baikal (Figure
430 3). Decreasing $\delta^{30}\text{Si}_{\text{diatom}}$ compositions and modelled DSi utilisation may further corroborate this
431 reduction in productivity, leading to the interpretation of reduced DSi demand (due to both reduced
432 productivity and the prevalence of smaller diatom species) (Figure 5). Overall we propose conditions
433 less favorable for larger spring blooming species (e.g. *S. grandis*). In particular, overall reduced
434 productivity is attributed to weaker spring convective mixing, the breakdown in thermal driven
435 stratification and a reduction in the overall growing season (increased ice cover duration) consistent with
436 the move to cooler conditions in the region (Figure 5).

437

438 Superimposed on these trends is a minimum in $\delta^{18}\text{O}_{\text{diatom}}$ compositions between c. 120.5 and 119.7 ka
439 BP (Figure 3), which Mackay et al. (2013) attribute to a cold perturbation in the Lake Baikal region (an
440 increase in Siberian High intensity; Tarasov et al., 2005) with increased snowmelt contributions and a
441 reduction in primary productivity (Fietz et al., 2007; Prokopenko et al., 2006; Rioual and Mackay, 2005).
442 Similarly, $\delta^{30}\text{Si}_{\text{diatom}}$ signatures also show a small (although within analytical uncertainty) decline, which
443 could be reflecting reduced diatom productivity during this cold event and therefore low DSi uptake (and
444 low modelled DSi supply) (Figures 4, 5). Interestingly, S/I ratios and HI increase after c. 120 ka BP
445 (Figure 4), which points to an increase in chemical weathering (intensity) in the Lake Baikal catchment
446 (e.g. towards supply-limited weathering regimes, indicative of higher river $\delta^{30}\text{Si}_{\text{DSi}}$), although as there
447 are no large changes in $\delta^{30}\text{Si}_{\text{diatom}}$ compositions after this time, we again suggest that isotopically altered
448 source waters to the lake have not had a confounding impact in driving $\delta^{30}\text{Si}_{\text{diatom}}$ signatures after this
449 time.

450

451 After c. 117.2 ka BP benthic diatom species increase in relative abundance (Rioual and Mackay, 2005).
452 This, along with a sharp fall in diatom BVAR and Chlorophyll-*a* concentrations (Fietz et al., 2007),
453 points to a reduction in pelagic productivity indicative of a switch to a much colder climate after this
454 time, coincident with a continued decline in summer insolation, a shift to increased steppe biomes scores
455 (Figure 4) and reduced mean summer temperatures (Tarasov et al., 2007; Tarasov et al., 2005), all while
456 ice sheet growth occurred in the Northern Hemisphere (Kukla et al., 2002).

457

458 **5. Conclusions**

459 Here we present the first application of $\delta^{30}\text{Si}_{\text{diatom}}$ in the palaeorecord at Lake Baikal and present it as a
460 proxy for both nutrient availability and demand over the Last Interglacial (MIS 5e). Overall, diatom
461 productivity is significantly higher in MIS 5e compared to the Holocene. In tandem with other published
462 productivity indicators from core CON-01-603-2, data point to an early interglacial stage of high DSi
463 demand by diatoms, although low nutrient conditions, in response to regional climate warming,
464 catchment vegetation and weathering regime changes. After c. 124 ka BP data suggest a move to higher
465 nutrient supply, although we attribute this to an increase in spring convective mixing based on overall
466 reconstructions of a stable Lake Baikal catchment (e.g. weathering indices and vegetation). We propose
467 complex within-lake conditions over the duration of MIS 5e, based on the variability in diatom nutrient
468 uptake and surface water nutrient availability (e.g. driven by changes in lake ice duration and turbulent
469 convective mixing). Unlike the earlier interpretative palaeoproductivity models based on BSi data alone,
470 we derive a more nuanced reconstruction highlighting that more caution should be taken to understand
471 fully the mechanisms at play during both inter- and intra-interglacial/glacial climates. This will better
472 inform the sensitivity and response of Lake Baikal to climate change both in the past and under future
473 anthropogenic and climate pressures.

474

475

476 **Acknowledgements:**

477 This work was supported by the Natural Environmental Research Council [grant number
478 NE/J00829X/1]. AWM acknowledges contributions from the EU FPV Project “CONTINENT” (Ref:
479 EKV2-2000-00057), for funding previous Last Interglacial studies on Lake Baikal.

480 **References:**

481

482 Alleman, L.Y., Cardinal, D., Cocquyt, C., Plisnier, P.D., Descy, J.P., Kimirei, I., Sinyinza, D., André,
483 L., 2005. Silicon isotopic fractionation in Lake Tanganyika and its main tributaries. *J. Great Lakes Res.*
484 31, 509-519

485 Bouchez, J., Gaillardet, J., von Blackenburg, F., 2014. Weathering intensity in lowland river basins:
486 from the Andes to the Amazon mouth. *Procedia Earth Planetary Sciences* 10, 280-286

487 Cardinal, D., Alleman, L.Y., de Jong, J., Ziegler, K., André, L., 2003. Isotopic composition of silicon
488 measured by multicollector plasma source mass spectrometry in dry plasma mode. *J. Anal. At.*
489 *Spectrom.* 18, 213-218. doi: 10.1039/B210109b

490 Charlet, F., Fagel, N., De Batist, M., Hauregard, F., Minnebo, B., Meischner, D., SONIC Team., 2005.
491 Sedimentary dynamics on isolated highs in Lake Baikal: evidence from detailed high-resolution
492 geophysical data and sediment cores. *Global Planet. Change* 46, 125-144. doi:
493 10.1016/J.Gloplacha.2004.11.009

494 De La Rocha, C.L., Brzezinski, M.A., DeNiro, M.J., 1997. Fractionation of silicon isotopes by marine
495 diatoms during biogenic silica formation. *Geochim. Cosmochim. Acta* 61, 5051-5056. doi:
496 10.1016/s0016-7037(97)00300-1

497 Demarest, M.S., Brzezinski, M.A., Beucher, C.P., 2009. Fractionation of silicon isotopes during
498 biogenic silica dissolution. *Geochim. Cosmochim. Acta* 73, 5572-5583. doi:10.1016/j.gca.2009.06.019

499 Demory, F., Nowaczyk, N.R., Witt, A., Oberhansli, H., 2005a. High-resolution magneto stratigraphy of
500 late quaternary sediments from Lake Baikal, Siberia: timing of intracontinental paleoclimatic
501 responses. *Global Planet. Change* 46, 167-186. doi: 10.1016/j.gloplacha.2004.09.016

502 Demory, F., Oberhansli, H., Nowaczyk, N.R., Gottschalk, M., Wirth, R., Naumann, R., 2005b. Detrital
503 input and early diagenesis in sediments from Lake Baikal revealed by rock magnetism. *Global Planet.*
504 *Change* 46, 145-166. doi:10.1016/j.gloplacha.2004.11.010

505 Dodson, S.I., Arnott, S.W., Cottingham, K.L., 2000. The relationship in lake communities between
506 primary productivity and species richness. *Ecology* 81, 2662-2679

507 Fagel, N., Alleman, L.Y., Granina, L., Hatert, F., Thamo-Bozso, E., Cloots, R., André, L., 2005.
508 Vivianite formation and distribution in Lake Baikal sediments. *Global Planet. Change* 46, 315-336. doi:
509 10.1016/J.Gloplacha.2004.09.022

510 Fagel, N., Boes, X., 2008. Clay-mineral record in Lake Baikal sediments: The Holocene and Late
511 Glacial transition. *Palaeogeography Palaeoclimatology Palaeoecology* 259, 230-243.
512 doi:10.1016/j.palaeo.2007.10.009

513 Fagel, N., Mackay, A.W., 2008. Weathering in the Lake Baikal watershed during the Kazantsevo
514 (Eemian) interglacial: Evidence from the lacustrine clay record. *Palaeogeography Palaeoclimatology*
515 *Palaeoecology* 259, 244-257. doi: 10.1016/J.Palaeo.2007.10.011

516 Fietz, S., Nicklisch, A., Oberhansli, H., 2007. Phytoplankton response to climate changes in Lake
517 Baikal during the Holocene and Kazantsevo Interglacials assessed from sedimentary pigments. *J.*
518 *Paleolimnol.* 37, 177-203. doi: 10.1007/s10933-006-9012-y

519 Fontorbe, G., De La Rocha, C.L., Chapman, H.J., Bickle, M.J., 2013. The silicon isotopic composition
520 of the Ganges and its tributaries. *Earth. Planet. Sci. Lett.* 381, 21-30. doi: 10.1016/J.Epsl.2013.08.026

521 Frings, P.J., Clymans, W., Fontorbe, G., De La Rocha, C.L., Conley, D.J., 2016. The continental Si
522 cycle and its impact on the ocean Si isotope budget. *Chem. Geol.* 425, 12-36. doi:
523 10.1016/j.chemgeo.2016.01.020

- 524 Frings, P.J., Clymans, W., Fontorbe, G., Gray, W., Chakrapani, G.J., Conley, D.J., De La Rocha, C.,
525 2015. Silicate weathering in the Ganges alluvial plain. *Earth. Planet. Sci. Lett.* 427, 136-148.
526 doi:10.1016/j.epsl.2015.06.049
- 527 Fripiat, F., Cavagna, A.J., Dehairs, F., Speich, S., André, L., Cardinal, D., 2011. Silicon pool dynamics
528 and biogenic silica export in the Southern Ocean inferred from Si-isotopes. *Ocean Sci.* 7, 533-547.
529 doi:10.5194/os-7-533-2011
- 530 Gaillardet, J., Dupré, B., Louvat, P., Allègre, C.J., 1999. Global silicate and CO₂ consumption rates
531 deduced from the chemistry of large rivers. *Chem. Geol.* 159, 3-30
- 532 Georg, R.B., Reynolds, B.C., Frank, M., Halliday, A.N., 2006. New sample preparation techniques for
533 the determination of Si isotopic compositions using MC-ICP-MS. *Chem. Geol.* 235, 95-104. doi:
534 10.1016/J.Chemgeo.2006.06.006
- 535 Granoszewski, W., Demske, D., Nita, M., Heumann, G., Andreev, A., 2005. Vegetation and climatic
536 variability during the Last interglacial evidenced in the pollen record from Lake Baikal. *Global Planet.*
537 *Change* 46, 187-198
- 538 Horn, M.G., Beucher, C.P., Robinson, R.S., Brzezinski, M.A., 2011. Southern ocean nitrogen and
539 silicon dynamics during the last deglaciation. *Earth. Planet. Sci. Lett.* 310, 334-339. doi:
540 10.1016/j.epsl.2011.08.016
- 541 Hughes, H.J., Delvigne, C., Korntheuer, M., de Jong, J., André, L., Cardinal, D., 2011. Controlling the
542 mass bias introduced by anionic and organic matrices in silicon isotopic measurements by MC-ICP-
543 MS. *J. Anal. At. Spectrom.* 26, 1892-1896. doi: 10.1039/C1ja10110b
- 544 Hughes, H.J., Sondag, F., Santos, R.V., André, L., Cardinal, D., 2013. The riverine silicon isotope
545 composition of the Amazon Basin. *Geochim. Cosmochim. Acta* 121, 637-651. doi:
546 10.1016/j.gca.2013.07.040
- 547 Jewson, D.H., Granin, N.G., Gnatovsky, R.Y., Lowry, S.F., Teubner, K., 2015. Coexistence of two
548 *Cyclotella* diatom species in the plankton of Lake Baikal. *Freshwat. Biol.* 60, 2113-2126. doi:
549 10.1111/fwb.12636
- 550 Karabanov, E., Prokopenko, A.A., Williams, D., Khursevich, G., 2000. Evidence for mid-Eemian
551 cooling in continental climatic record from Lake Baikal. *J. Paleolimnol.* 23, 365-371
- 552 Kukla, G.J., Bender, M.L., de Beaulieu, J.L., Bond, G., Broecker, W.S., Cleveringa, P., Gavin, J.E.,
553 Herbert, T.D., Imbrie, J., Jouzel, J., Keigwin, L.D., Knudsen, K.L., McManus, J.F., Merkt, J., Muhs,
554 D.R., Muller, H., Poore, R.Z., Porter, S.C., Seret, G., Shackleton, N.J., Turner, C., Tzedakis, P.C.,
555 Winograd, I.J., 2002. Last interglacial climates. *Quatern. Res.* 58, 2-13. doi: 10.1006/qres.2002.2316
- 556 Lydolph, P.E., 1977. *Geography of the USSR*. Elsevier, The Hague.
- 557 Mackay, A., 2007. The paleoclimatology of Lake Baikal: A diatom synthesis and prospectus. *Earth*
558 *Science Reviews* 82, 181-215
- 559 Mackay, A.W., Swann, G.E.A., Fagel, N., Fietz, S., Leng, M.J., Morley, D., Rioual, P., Tarasov, P.,
560 2013. Hydrological instability during the Last Interglacial in central Asia: a new diatom oxygen isotope
561 record from Lake Baikal. *Quaternary Science Reviews* 66, 45-54. doi: 10.1016/j.quascirev.2012.09.025
- 562 Martin-Jezequel, V., Hildebrand, M., Brzezinski, M.A., 2000. Silicon metabolism in diatoms:
563 Implications for growth. *J. Phycol.* 36, 821-840. doi: 10.1046/J.1529-8817.2000.00019.X
- 564 Milligan, A.J., Varela, D.E., Brzezinski, M.A., Morel, F.O.M.M., 2004. Dynamics of silicon
565 metabolism and silicon isotopic discrimination in a marine diatom as a function of *p*CO₂. *Limnol.*
566 *Oceanogr.* 49, 322-329

- 567 Morley, D.W., Leng, M.J., Mackay, A.W., Sloane, H.J., Rioual, P., Sturm, M., 2004. Cleaning of lake
568 sediment samples for diatom oxygen isotope analysis. *J. Paleolimnol.* 31, 391-401
- 569 Opfergelt, S., Eiriksdottir, E.S., Burton, K.W., Einarsson, A., Siebert, C., Gislason, S.R., Halliday,
570 A.N., 2011. Quantifying the impact of freshwater diatom productivity on silicon isotopes and silicon
571 fluxes: Lake Myvatn, Iceland. *Earth. Planet. Sci. Lett.* 305, 73-82. doi: 10.1016/j.epsl.2011.02.043
- 572 Oppo, D.W., McManus, J.F., Cullen, J.L., 2006. Evolution and demise of the Last Interglacial warmth
573 in the subpolar North Atlantic. *Quaternary Science Reviews* 25, 3268-3277. doi:
574 10.1016/j.quascirev.2006.07.006
- 575 Panizzo, V.N., Roberts, S., Swann, G.A.A., McGowan, S., Mackay, A.W., Vologina, E., Pashley, V.,
576 Horstwood, M.S.A., In review. Spatial differences in dissolved silicon utilisation in Lake Baikal,
577 Siberia: disentangling the effects of high diatom biomass events and eutrophication. *Limnol. Oceanogr.*
- 578 Panizzo, V.N., Swann, G.E., Mackay, A.W., Vologina, E.G., Pashley, V.H., Horstwood, M.S.A., 2017.
579 Constraining modern-day silicon cycling in Lake Baikal. *Global Biogeochem. Cycles* 2017, 556-574.
580 doi: 10.1002/2016GB005518
- 581 Panizzo, V.N., Swann, G.E.A., Mackay, A.W., Vologina, E., Sturm, M., Pashley, V., Horstwood,
582 M.S.A., 2016. Insights into the transfer of silicon isotopes into the sediment record. *Biogeosciences* 13,
583 147-157. doi: 10.5194/bg-13-147-2016
- 584 Past Interglacials Working Group of PAGES., 2016. Interglacials of the last 800,000 years. 54, 162-
585 219. doi:10.1002/2015RG000482
- 586 Popovskaya, G.I., 2000. Ecological monitoring of phytoplankton in Lake Baikal. *Aquat. Ecosyst.*
587 *Health Manage.* 3, 215-225
- 588 Popovskaya, G.I., Usol'tseva, M.V., Domysheva, V.M., Sakirko, M.V., Blinov, V.V., Khodzher, T.V.,
589 2015. The Spring Phytoplankton in the Pelagic Zone of Lake Baikal During 2007-2011. *Geogr. Natural*
590 *Resources* 36, 253-262. doi: 10.1134/s1875372815030051
- 591 Prokopenko, A.A., Hinnov, L.A., Williams, D.F., Kuzmin, M.I., 2006. Orbital forcing of continental
592 climate during the Pleistocene: a complete astronomically tuned climatic record from Lake Baikal, SE
593 Siberia. *Quaternary Science Reviews* 25, 3431-3457. doi: 10.1016/j.quascirev.2006.10.002
- 594 Prokopenko, A.A., Karabanov, E.B., Williams, D.F., Kuzmin, M.I., Shackleton, N.J., Crowhurst, S.J.,
595 Peck, J.A., Gvozdkov, A.N., King, J.W., 2001. Biogenic silica record of the Lake Baikal response to
596 climatic forcing during the Brunhes. *Quatern. Res.* 55, 123-132. doi: 10.1006/qres.2000.2212
- 597 Railsback, L.B., Gibbard, P.L., Head, M.J., Voarintsoa, N.R.G., Toucanne, S., 2015. An optimized
598 scheme of lettered marine isotope substages for the last 1.0 million years, and the climatostratigraphic
599 nature of isotope stages and substages. *Quaternary Science Reviews* 111, 94-106. doi:
600 10.1016/j.quascirev.2015.01.012
- 601 Reynolds, B.C., Aggarwal, J., Andre, L., Baxter, D., Beucher, C., Brzezinski, M.A., Engström, E.,
602 Georg, R.B., Land, M., Leng, M.J., Opfergelt, S., Rodushkin, I., Sloane, H., van den Boorn, S.H.J.M.,
603 Vroon, P.Z., Cardinal, D., 2007. An inter-laboratory comparison of Si isotope reference materials. *J.*
604 *Anal. At. Spectrom.* 22, 561-568
- 605 Rioual, P., Mackay, A.W., 2005. A diatom record of centennial resolution for the Kazantsevo
606 Interglacial stage in Lake Baikal (Siberia). *Global Planet. Change* 46, 199-219. doi:
607 10.1016/j.gloplacha.2004.08.002
- 608 Ryves, D.B., Jewson, D.H., Sturm, M., Battarbee, R.W., Flower, R.J., Mackay, A.W., Granin, N.G.,
609 2003. Quantitative and qualitative relationships between planktonic diatom communities and diatom
610 assemblages in sedimenting material and surface sediments in Lake Baikal, Siberia. *Limnol. Oceanogr.*
611 48, 1643-1661

- 612 Shimaraev, M.N., Granin, N.G., Zhdanov, A.A., 1993. Deep ventilation of Lake Baikal waters due to
613 spring thermal bars. *Limnological and Oceanography* 38, 1068-1072
- 614 Short, D.A., Mengel, J.G., Crowley, T.J., Hyde, W.T., North, G.R., 1991. Filtering of Milankovitch
615 Cycles by Earths Geography. *Quatern. Res.* 35, 157-173. doi: 10.1016/0033-5894(91)90064-C
- 616 Stumm, W., Wollast, R., 1990. Coordination chemistry of weathering: kinetics of the surface-
617 controlled dissolution of oxide minerals. *Review of Geophysics* 28, 53-69
- 618 Sun, X.L., Andersson, P.S., Humborg, C., Pastuszak, M., Morth, C.M., 2013. Silicon isotope
619 enrichment in diatoms during nutrient-limited blooms in a eutrophied river system. *Journal of*
620 *Geochemical Exploration* 132, 173-180. doi: 10.1016/J.Gexplo.2013.06.014
- 621 Sutton, J.N., Varela, D.E., Brzezinski, M.A., Beucher, C.P., 2013. Species-dependent silicon isotope
622 fractionation by marine diatoms. *Geochim. Cosmochim. Acta* 104, 300-309. doi:
623 10.1016/J.Gca.2012.10.057
- 624 Tarasov, P., Bezrukova, E., Karabanov, E., Nakagawa, T., Wagner, M., Kulagina, N., Letunova, P.,
625 Abzaeva, A., Granoszewski, W., Riedel, F., 2007. Vegetation and climate dynamics during the
626 Holocene and Eemian interglacials derived from Lake Baikal pollen records. *Palaeogeography,*
627 *Palaeoclimatology, Palaeoecology* 252, 440-457. doi: 10.1016/j.palaeo.2007.05.002
- 628 Tarasov, P., Granoszewski, W., Berzukova, Y.V., Brewer, S., Nita, M., Abzaeva, A., Oberhaensli, H.,
629 2005. Quantitative reconstruction of the Last Interglacial climate based on the pollen record from Lake
630 Baikal, Russia. *Clim. Dyn.* 25, 625-637
- 631 Varela, D.E., Pride, C.J., Brzezinski, M.A., 2004. Biological fractionation of silicon isotopes in
632 Southern Ocean surface waters. *Global Biogeochem. Cycles* 18. doi: 10.1029/2003gb002140
633
- 634 Velichko, A.A., Borisova, O.K., Gurtovaya, Y.Y., Zelikson, E.M., 1991. Climatic rhythm of the last
635 interglacial in northern Eurasia. *Quaternary International* 10-12, 191-213
- 636 Williams, D.F., Kuzmin, M.I., Prokopenko, A.A., Karabanov, E.B., Khursevich, G.K., Bezrukova,
637 E.V., 2001. The Lake Baikal drilling projects in the context of a global lake drilling initiative.
638 *Quaternary International* 80-1, 3-18. doi: 10.1016/S1040-6182(01)00015-5
639
- 640